SCIENTIFIC REPORTS

OPEN

SUBJECT AREAS:
AUTOPHAGY
PRIONS

Received
3 January 2014

Accepted
4 March 2014

Published
28 March 2014

Correspondence and requests for materials should be addressed to D.I. (dishi@nagasaki-u.ac.jp)

Increased expression of p62/SQSTM1 in prion diseases and its association with pathogenic prion protein

Takujiro Homma[1], Daisuke Ishibashi[1], Takehiro Nakagaki[1], Katsuya Satoh[1], Kazunori Sano[1], Ryuichiro Atarashi[1,2] & Noriyuki Nishida[1]

[1]Department of Molecular Microbiology and immunology, Graduate School of Biomedical sciences, Nagasaki University, Nagasaki 852-8523, Japan, [2]Nagasaki University Research Centre for Genomic Instability and Carcinogenesis, Nagasaki 852-8523, Japan.

Prion diseases are neurodegenerative disorders characterized by the aggregation of abnormally folded prion protein (PrP^{Sc}). In this study, we focused on the mechanism of clearance of PrP^{Sc}, which remains unclear. p62 is a cytosolic protein known to mediate both the formation and degradation of aggregates of abnormal proteins. The levels of p62 protein increased in prion-infected brains and persistently infected cell cultures. Upon proteasome inhibition, p62 co-localized with PrP^{Sc}, forming a large aggregate in the perinuclear region, hereafter referred to as PrP^{Sc}-aggresome. These aggregates were surrounded with autophagosome marker LC3 and lysosomes in prion-infected cells. Moreover, transient expression of the phosphomimic form of p62, which has enhanced ubiquitin-binding activity, reduced the amount of PrP^{Sc} in prion-infected cells, indicating that the activation of p62 could accelerate the clearance of PrP^{Sc}. Our findings would thus suggest that p62 could be a target for the therapeutic control of prion diseases.

Prion diseases are fatal neurodegenerative disorders associated with the conformational conversion of normal cellular prion protein (PrP^{C}) to β-sheet-rich pathogenic prion protein (PrP^{Sc})[1]. The histopathological hallmarks of prion diseases are spongiform changes, marked neuronal loss and gliosis. In addition, large amyloids composed of PrP^{Sc} can be observed in most affected brains[2,3]. However, the role of these aggregates in the pathogenesis remains to be elucidated. Although the formation of neuronal inclusion bodies might be a protective reaction of cells to reduce the levels of toxic forms of abnormal proteins[4], it was reported that β-sheet-rich PrP inhibits the catalytic activity of proteasomes[5], leading to a disruption of protein homeostasis. As the ubiquitin-proteasome system (UPS) is essential in the degradation of abnormal proteins, its impairment has been implicated in the "conformational" disorders such as Huntington's disease, Parkinson's disease and Alzheimer's disease[6], in which misfolded proteins are known to make aggregates. As the aggregates contain polyubiquitinated proteins and also proteasomes, their build-up promotes a vicious cycle in which the UPS becomes still further hampered[7]. When the UPS is disrupted, ubiquitinated proteins are transported to the perinuclear region via a dynein-dependent retrograde transport system, where they form large complexes termed aggresomes[8–10]. p62, which was originally identified as adapter proteins involved in multiple cell-signaling pathways, has recently been reported to function in the formation of aggresomes. It has also been shown that p62 binds to ubiquitin and interacts with an autophagosomal membrane protein, microtubule-associated protein 1 light chain 3 (LC3-II)[11–14]. Thus, aggregated proteins sequestered by p62 are degraded through the autophagolysosomal pathway[15,16]. Interestingly, p62 has also been found in neuronal inclusion bodies with ubiquitinated protein aggregates in Alzheimer's disease, Pick's disease, dementia with Lewy bodies, Parkinson's disease, frontotemporal lobar degeneration, and amyotrophic lateral sclerosis (ALS)[17–22]. It has been reported that PrP^{Sc} degradation is accelerated by activation of autophagy[23–25], however the mechanism of clearance of PrP^{Sc} aggregates has not been fully elucidated. In this study, we investigated the role of p62 in prion-infected cell culture models and found that p62 was co-localized with PrP^{Sc}-aggresomes, and that the activation of p62 was able to reduce the accumulation of PrP^{Sc}.

Results

Up-regulation of p62 was observed following prion infection. To investigate the expression levels of p62 protein in prion-infected mice, we intracerebrally inoculated 22 L prions into ddY mice (n = 3) and

examined the levels of p62 protein in the brains of terminally sick mice by immunoblotting. Significantly up-regulated p62 was observed in the brains of 22L-inoculated mice, compared with that of the control mice (Fig. 1a). Up-regulated LC3-II was also observed, suggesting the involvement of autophagic degradation.

We next intraperitoneally inoculated 263 K prions into Syrian hamsters and examined the levels of p62 protein in the brains of terminally sick hamsters by immunoblotting. The levels of p62 also increased in the brains of 263K-inoculated hamsters, compared with those of the control hamsters (Fig. 1b). The presence of PrP^{Sc} was identified in all infected brains.

For further experiments, we used ScN2a58 cells, persistently 22L-infected N2a58 cells, containing high amounts of PrP^{Sc}. Immunoblotting revealed that the levels of p62 protein also increased in ScN2a58 cells compared with uninfected N2a58 cells (Fig. 2a). Moreover, the levels of p62 mRNA also significantly increased in ScN2a58 cells (Fig. 2b).

As microglia are known to play a major role in initiating the pathological changes in prion disease, we investigated the effects of prion infection on p62 using a microglial cell line (MG20). We added 0.1% brain homogenates from 22L-infected mice (22 L BH) or normal mice (nBH) to MG20 cells. After serial passages, the presence of PrP^{Sc} and up-regulation of p62 were identified in the 22L-infected cells from passage 3 (Fig. 2c), indicating that the phenomenon was not neuron-specific. Taken together, these data showed that up-regulation of p62 subsequently occurs *in vivo* and *in vitro* due to prion infection.

p62 co-localizes with PrP^{Sc} in prion-infected cells. It has been reported that PrP^{C} is retrogradely transported from the endoplasmic reticulum (ER) and accumulates in the cytosol as protease-resistant and detergent-insoluble PrP upon proteasome inhibition[26], and that aggregates may contain ubiquitinated proteins[27]. Another reports suggest that some of the PrP aggregates contain uncleaved signal peptides after proteasome inhibition, indicating the existence of ERAD-independent mechanism in which PrP fails to translocate into the ER lumen[28–30]. To determine whether such PrP aggregates are recognized by p62, we investigated the subcellular localization of total PrP and p62 in N2a58 and ScN2a58 cells by immunofluorescence staining. Under normal conditions, immunofluorescence for total PrP was greater in ScN2a58 cells than in N2a58 cells [Fig. 3a, MG132 (-)]. In both cell types, endogenous p62 was distributed throughout the cytoplasm [Fig. 3a, MG132 (-)], consistent with previous observations[11,14,31]. When we treated N2a58 and ScN2a58 cells with a chemical proteasome inhibitor, MG132 (10 μM, 24 h) to see how the impairment of UPS affects the distribution of PrP and p62, singular p62-containing inclusions were frequently induced at the perinuclear region in both cell types [Fig. 3a, MG132 (+)]. Interestingly, total PrP was dramatically localized to p62 complex in ScN2a58 cells, suggesting that misfolded PrP tends to promote the formation of large aggresomes in prion-infected cells. To investigate whether PrP^{Sc} is sequestered in the p62 complex, we visualized PrP^{Sc} by immunofluorescence staining in combination with prior treatment with guanidium salts, which significantly increases the PrP^{Sc} signal[32]. After treatment with guanidine thiocyanate, PrP^{Sc} was detected in ScN2a58 cells, but not in N2a58 cells, and partially co-localized with endogenous p62 (Fig. 3b). Upon proteasome inhibition, a large PrP aggregate formed in the perinuclear region, hereafter referred to as "PrP^{Sc}-aggresome", and importantly, p62 relocalized to PrP^{Sc}-aggresome. (Fig. 3b).

We next investigated whether the knockdown of p62 affects the formation of PrP^{Sc}-aggresome. We treated p62-specific siRNA or control siRNA to ScN2a58 cells (50 nM, 48 h), following MG132

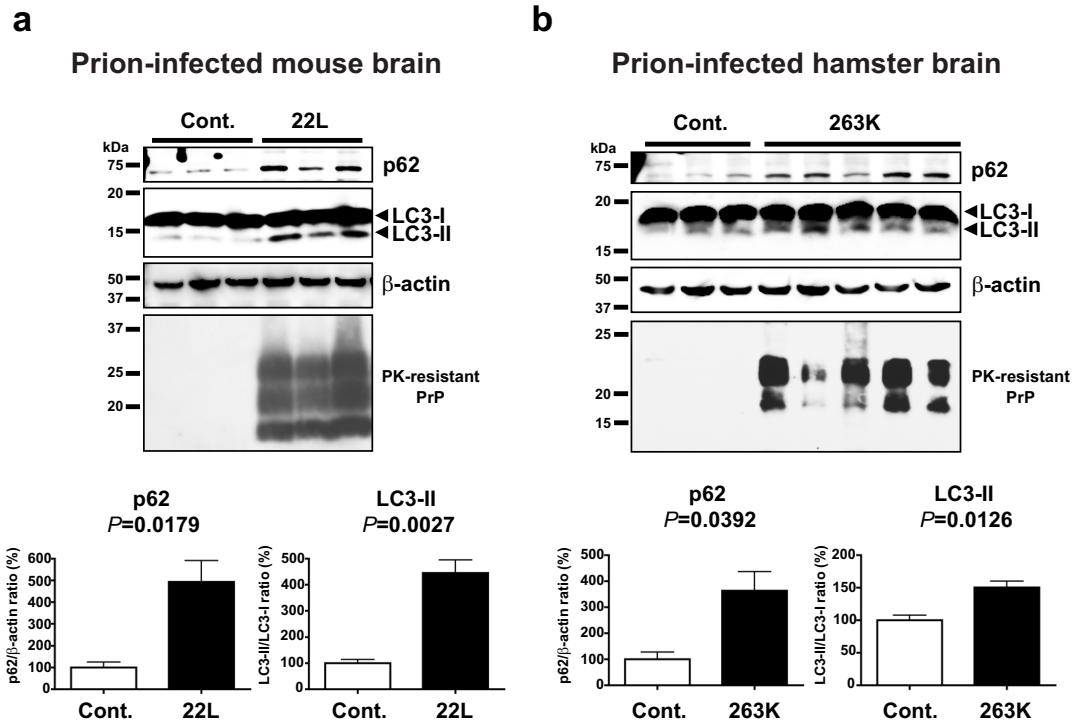

Figure 1 | Up-regulation of p62 in prion-infected brains. (a) The levels of p62 protein in the brains of control (Cont.) or 22 L inoculated ddY mice (n = 3, per group). The amount of p62, LC3 and PK-resistant PrP (M20) was analyzed by immunoblotting. β-actin was used as a loading control. Statistical significance was evaluated using Student's *t*-test. (b) The levels of p62 protein in the brains of control (Cont.) or 263 K inoculated Syrian hamsters. The amount of p62, LC3 and PK-resistant PrP (3F4) was analyzed by immunoblotting. β-actin was used as a loading control. Statistical significance was evaluated using Student's *t*-test.

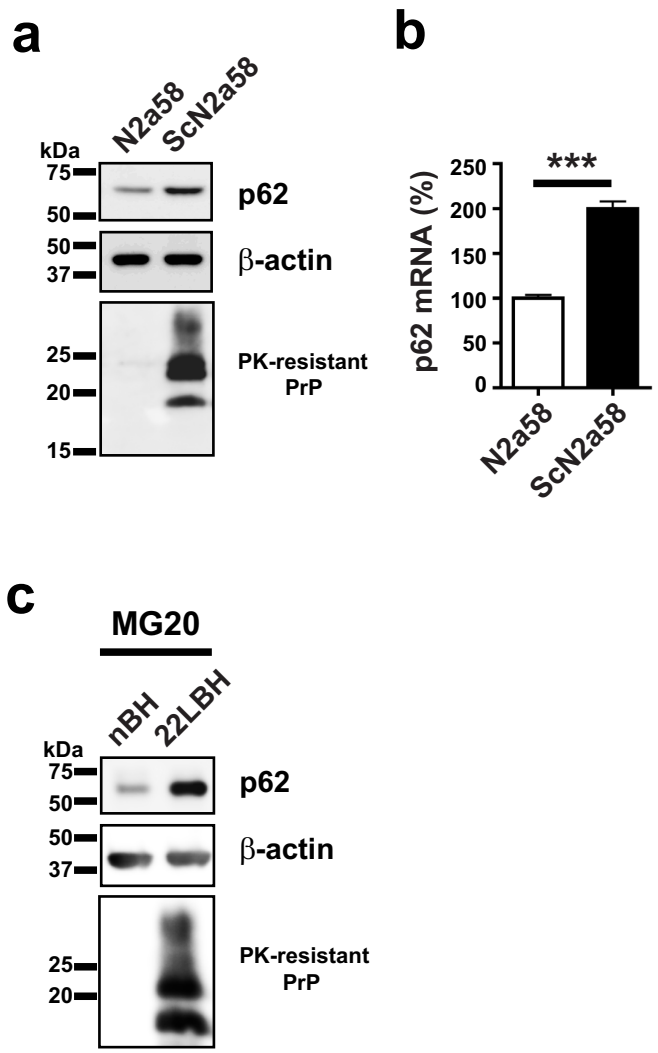

Figure 2 | Up-regulation of p62 in prion-infected cell cultures. (a) The levels of p62 protein in N2a58 and ScN2a58 cells. The amount of p62 and PK-resistant PrP (M20) was analyzed by immunoblotting. β-actin was used as a loading control. (b) The levels of p62 mRNA in N2a58 and ScN2a58 cells were analyzed by Real time PCR. Asterisks indicate statistically significant differences (***, $P < 0.001$; a two-tailed Student's *t*-test; $n = 8$). (c) The levels of p62 protein in *de novo* infection of 22 L prion strain in MG20 cells. After the treatment of 0.1% 22 L BH or nBH to MG20 cells, the amount of p62 and PK-resistant PrP (M20) was analyzed by immunoblotting. β-actin was used as a loading control.

treatment (10 μM, 24 h). As expected, in control siRNA-treated cells, the PrP^{Sc}-aggresomes formed after proteasome inhibition (Fig. 4). In contrast, in p62 siRNA-treated cells, in which p62 fluorescence was successfully decreased, PrP^{Sc}-aggresomes did not form, suggesting the presence of p62 to be crucial for PrP^{Sc}-aggresome formation.

p62 relocalized to PrP^{Sc}-aggresomes through ubiquitin-binding. p62 is known to interact with ubiquitinated proteins through its C-terminus ubiquitin-associated domain (UBA)[33]. To investigate whether or not the co-localization of p62 and PrP^{Sc} was dependent on the domain, we introduced expression vectors of HA-tagged p62 or UBA domain-deleted p62 (p62ΔUBA, missing amino acids 388–442) into ScN2a58 cells and visualized p62 and PrP^{Sc}. As expected, HA-tagged p62 relocalized to PrP^{Sc}-aggresomes upon proteasome inhibition (Fig. 5). In contrast, HA-tagged p62ΔUBA did not relocalize to PrP^{Sc}-aggresomes, suggesting that the UBA domain plays a critical role in p62 recruitment to PrP^{Sc}-aggresomes. The levels of p62 protein increased by MG132 (10 μM, 24 h), and ubiquitinated proteins with high-molecular-weight (HMW, ~250 kDa), which are likely to derive from the aggresomes, were evident in ScN2a58 cells (Fig. S1), suggesting that PrP^{Sc}-aggresomes contain large ubiquitinated proteins.

PrP is co-immunoprecipitated with p62. We next performed co-immunoprecipitation experiments using ScN2a58 cell lysates. Endogenous p62 was co-immunoprecipitated with anti-PrP antibody (SAF32) both without (Fig. S2, top left) and with proteasome inhibition (Fig. S2, top right). The presence of PrP in SAF32 immunoprecipitates was also identified in both lysates (Fig. S2, bottom).

p62-positive aggresomes in prion-infected cells are surrounded by lysosomes. We next investigated the localization of such aggresomes and lysosomes in ScN2a58 cells, and we showed that p62-positive aggresomes were surrounded by lysosomes (Fig. 6a). Similar result was obtained in PrP-positive aggresomes (Fig. 6b). We also observed that LC3 was concentrated in the aggresomes (Fig. 6c). These results suggest that such aggresomes are potentially degraded in lysosomes.

p62 is involved in the degradation of PrP^{Sc}. To investigate whether overexpression of p62 affects the degradation of PrP^{Sc}, a HA-tagged p62 was introduced into N2a58 cells or ScN2a58 cells, and the amount of PrP^{Sc} was analyzed. Transient expression of p62 had no effect on the amount the amount of PK-resistant PrP (Fig. 7a). It has been shown that the activity of p62 appears to be controlled by phosphorylation at serine 403 (S403) of the human p62 UBA domain due to enhancement of its affinity to polyubiquitin, promoting efficient autophagic degradation of ubiquitinated proteins[34]. To investigate whether phosphorylation of the UBA domain affects the clearance of PrP^{Sc}, a HA-tagged phosphomimic mutant, with the substitution of mouse p62 serine 405 for glutamate (corresponding to S403 in human p62) (Fig. 7b), was introduced into ScN2a58 cells and the amount of PrP^{Sc} was analyzed. Transient expression of phosphomimic p62-HA reduced the amount of PrP^{Sc} in ScN2a58 cells (Fig. 7c). To confirm whether the mutation enhanced the affinity between p62 and ubiquitinated proteins, the lysates from transfected cells were immunoprecipitated with anti-HA antibody, and ubiquitinated proteins in the immunoprecipitates were detected by immunoblotting. As expected, the amount of ubiquitinated proteins in phosphomimic p62 transfected cells was greater than those in mock or wild-type transfected cells (Fig. 7d). In addition, after the blocking of lysosomal degradation by ammonium chloride, phosphomimic p62 was largely localized in lysosomes (Fig. S3). Taken together, these results suggest that phosphomimic p62 accelerated the clearance of PrP^{Sc} in lysosomes.

Discussion

Our study revealed the following. (1) p62 increased in association with prion-infection in cell cultures and brains (Fig. 1 and 2); (2) Large PrP^{Sc} aggregates encircled by p62 form when the UPS is disrupted (Fig. 3b); (3) The interaction of p62 with polyubiquitin is crucial to the formation of PrP^{Sc}-aggresomes (Fig. 5); and (4) the constitutively active form of p62 could reduce the amount of PrP^{Sc} in infected cells (Fig. 7c). These findings suggest that p62-mediated aggresome-formation could be important in the host-defense response against prion infection.

Contrary to our data, Xu *et al*[35] previously reported that the levels of p62 protein and ubiquitinated proteins were decreased in the brains of 263K-infected hamsters. This discrepancy is unknown, but may be related to the differences in the experimental conditions.

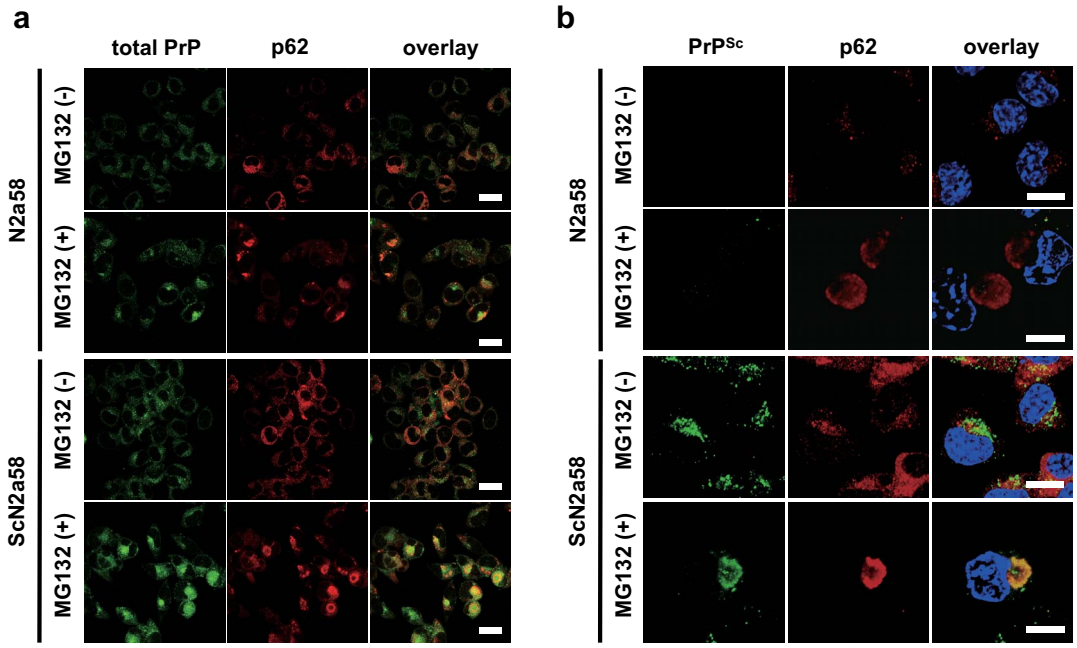

Figure 3 | Co-localization of p62 and PrP after proteasome inhibition. (a) Total PrP (SAF32: green) and p62 (red) were visualized in N2a58 and ScN2a58 cells with (+) or without (−) MG132 (10 μM, 24 h). Bars: 20 μm. (b) After the treatment of guanidine thiocyanate, PrP^{Sc} (SAF61: green) and p62 (red) were visualized in N2a58 and ScN2a58 cells with (+) or without (−) MG132 (10 μM, 24 h). Bars: 20 μm.

Several different reports have described that the levels of p62 protein are known to be increased when proteasome function is inhibited[18,20,36]. In prion-infected animal brains, proteasome activities are known to be reduced, and it has been clearly evidenced that PrP^{Sc} binds to the 20S core particle of proteasomes *in vitro*[37] and inhibit proteasome activity in neurons[5]. Actually, it has recently been reported that transcription factor NF-E2-related factor 2 (Nrf2), which enhances the expression of p62[38], was activated when the UPS is impaired[39]. Furthermore, as p62 interacts with Keap1, which regulates the turnover of Nrf2, the up-regulated p62 may competitively inhibit the Nrf2–Keap1 interaction, resulting in stabilization of Nrf2 followed by transcriptional activation of p62[40]. This positive feedback loop may contribute to the up-regulation of p62 demonstrated in this study in the large PrP^{Sc}-aggresomes forming in infected cells when proteasomes were inhibited by MG132. These findings suggest that direct inhibition of the UPS by PrP^{Sc} prompts the up-regulation of p62 as a compensatory mechanism of the UPS in prion diseases.

It is well known that p62 can bind to polyubiquitinated proteins and play a role in the degradation of misfolded proteins such as the polyglutamine-expanded huntingtin[34]. Relatively large PrP^{Sc}-aggresomes encircled by p62 were observed in infected cells when the UPS was disrupted, suggesting that p62 mediates PrP^{Sc}-aggresome formation (Fig. 3b). Because it is not clear whether PrP^{Sc} itself is ubiquitinated or not, we cannot exclude the possibility that p62 binds indirectly with PrP^{Sc}. It is likely that the formation of p62-PrP^{Sc}

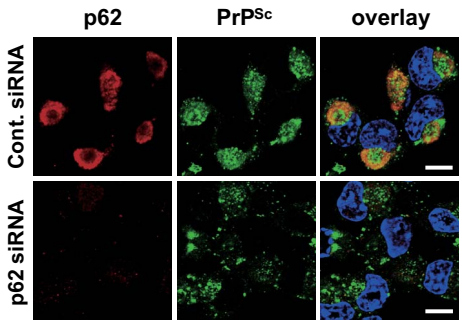

Figure 4 | Knockdown of p62 disrupts the formation of PrP^{Sc}-aggresome. ScN2a58 cells were treated with p62-specific siRNA or control siRNA (50 nM, 48 h), following MG132 treatment (10 μM, 24 h). After the treatment of guanidine thiocyanate, PrP^{Sc} (SAF61: green) and p62 (red) were visualized. Bars: 20 μm.

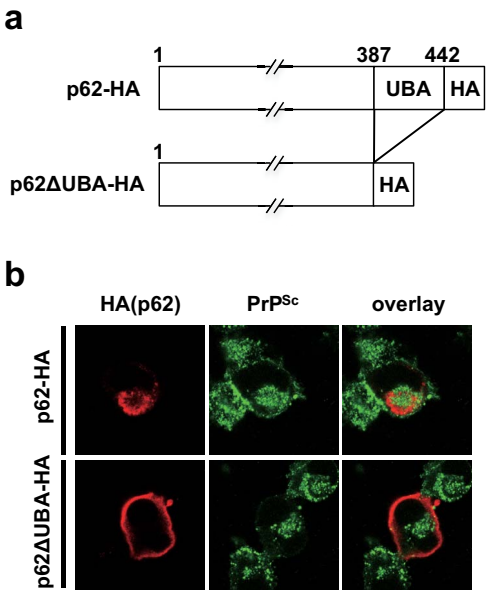

Figure 5 | UBA of p62 is required for the formation of PrP^{Sc}-aggresome. (a) Scheme of HA-tagged p62 or UBA domain-deleted p62 (p62ΔUBA, missing amino acids 388–442). (b) HA-tagged p62 or p62ΔUBA expression vectors were transiently expressed in ScN2a58 cells for 48 h, following with MG132 (10 μM, 24 h). After the treatment of guanidine thiocyanate, PrP^{Sc} (SAF61: green) and HA (red) were visualized.

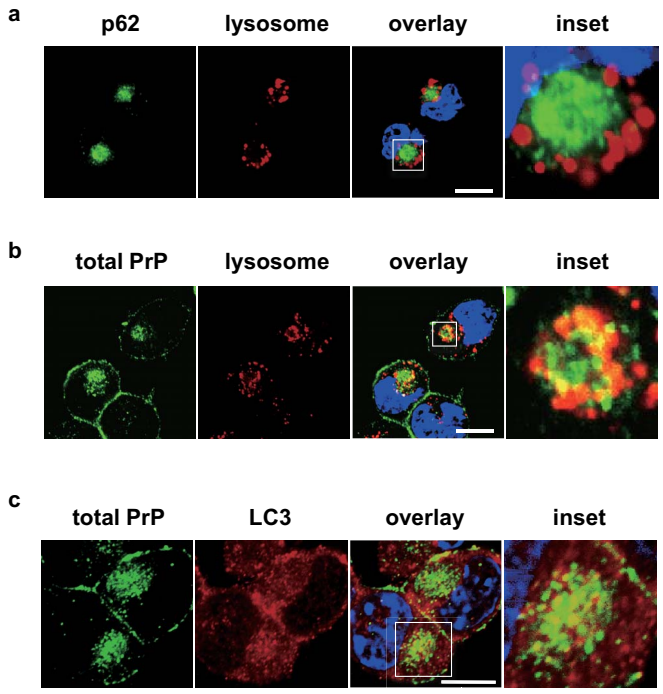

Figure 6 | Aggresomes in prion-infected cells are surrounded by lysosomes. (a) p62 (green) and lysosome (red) were visualized in ScN2a58 cells treated with MG132 (10 μM, 24 h). Bars: 20 μm. (b) Total PrP (SAF32: green) and lysosome (red) were visualized in ScN2a58 cells treated with MG132 (10 μM, 24 h). Bars: 20 μm. (c) Total PrP (SAF32: green) and LC3 (red) were visualized in ScN2a58 cells treated with MG132 (10 μM, 24 h). Bars: 20 μm.

complexes is dependent upon the presence of other ubiquitinated proteins in the PrP^{Sc}-aggresomes because these are often observed in PrP plaques in CJD brains[41,42]. Based on the fact that the phosphomimic p62, which has enhanced ubiquitin-binding activity, promoted the clearance of PrP^{Sc} (Fig. 7c), we came to the conclusion that activation of p62 is important for the efficient clearance of PrP^{Sc}.

It has been reported that p62 and its association with ubiquitin is involved in the clearance of neuronal inclusion bodies such as α-synuclein[43], polyglutamine-expanded huntingtin[34] and androgen receptor[44], through the autophagy-lysosome pathway. In addition, it has very recently reported overexpression of p62 promotes the degradation of some mutant PrPs such as PrP-PG14, a PrP mutant with the extra nine-octapeptide insertion associated with genetic CJD and PrP-CYTO, a PrP mutant without signal peptide and GPI anchor[45]. In our study, we have provided evidence that overexpression of p62 promotes the degradation of pathogenic prion protein, although the effect is limited to phosphomimic form of p62. Taking into account that non-phosphorylated p62 has relatively low affinity for ubiquitin, phosphorylation of p62 is important for the efficient degradation.

In conclusion, disruption of the UPS may be involved in prion pathogenesis, while the enhancement of p62-activity is a possible therapeutic target for the induction of the autophagic clearance of pathogenic prion proteins.

Methods

Antibodies. Anti-p62/SQSTM1 (MBL, PM045), anti-β-actin (Sigma-Aldrich), anti-HA (Invitrogen), anti-ubiquitin (Santa Cruz Biotechnology, P4D1), anti-LC3B (Cell Signaling Technology, #2775), and anti-PrP (Santa Cruz Biotechnology, M20; SPI-Bio, SAF61 and SAF32; SIGNET, 3F4) antibodies were purchased from the indicated vendors. Horseradish peroxidase-conjugated anti-goat (Santa Cruz Biotechnology), anti-mouse and anti-rabbit IgG antibodies (GE Healthcare Life Sciences) were used for immunoblotting. Alexa Fluor® 488-conjugated anti–mouse IgG and Alexa Fluor® 594-conjugated anti–rabbit IgG antibodies (Invitrogen) were used for immunofluorescence analysis.

Cell cultures. The mouse neuroblastoma Neuro 2a cells were obtained from the American Type Culture Collection (CCL 131). N2a58 cells are mouse PrP^{C} overexpressing Neuro 2a cells, and ScN2a58 cells originated from N2a58 cells infected with a mouse-adapted scrapie strain, 22 L, as previously described[46,47]. The cells were cultured in Dulbecco's modified Eagle's medium (DMEM; Sigma-Aldrich) containing 10% heat-inactivated fetal bovine serum (FBS) and penicillin-streptomycin (Invitrogen). MG20 cells (a gift from Dr. Iwamaru), isolated from neonatal tga20 mice that overexpress mouse PrP^{C}[48], were cultured in DMEM containing 10% heat-inactivated FBS, penicillin-streptomycin, 2-mercapto-ethanol and insulin. All cultured cells were maintained at 37°C in 5% CO_2 in the biohazard prevention area of Nagasaki University.

Plasmids and siRNA. Mouse p62 open reading frame was amplified from N2a58 cDNA with primers of mp62-BamHI-F (5′-cgcggatccgcggttatggcgtcgttcacg-3′) and mp62-XhoI-R (5′-ccgctcgagtcattaagcgtaatctggaacatcgtatgggtacaatggtggagggtgctt-3′). UBA domain-deleted p62 (p62ΔUBA, missing amino acids 388–442) was amplified with primers of mp62-BamHI-F and mp62ΔUBA-XhoI-R (5′-ccgctcgagtcattaagcgtaatctggaacatcgtatgggtaatgtgggtatagggcagcttc-3′). phosphomimic p62 was amplified with primers of mp62 (S405E)-BamHI-F (5′-tcccagatgctggagatgggcttctctgat-3′) and mp62 (S405E)-XhoI-R (5′-atcagagaagcccatctccagcatctggga-3′). Amplified PCR fragments were inserted into the BamHI and XhoI sites of expression plasmid pcDNA3.1 (Invitrogen) and confirmed by sequential analysis. All plasmids were introduced by Lipofectamine LTX (Invitrogen) in prion-infected cells and analyzed 48 h after transfection. ON-TARGETplus small interference RNA (siRNA) against mouse p62 (J-047628-12-0005) was purchased from Thermo Scientific as well as the control ON-TARGETplus non-targeting siRNA (D-001810-01-05). Transfection with siRNAs was carried out with Lipofectamine 2000 (Invitrogen) according to the manufacturer's protocol.

Immunoblotting. Immunoblotting analysis was performed as previously described[49]. Briefly, samples were lysed with cold lysis buffer (50 mM Tris-HCl pH 7.5, 150 mM NaCl, 0.5% Triton X-100, 0.5% sodium deoxycholate, 2 mM EDTA) containing protease inhibitors (Nacalai Tesque, Inc., Kyoto, Japan) for 30 min at 4°C. After 10 min of centrifugation at 15,000 × g, the supernatant was collected, and the concentration of total protein was measured using BCA Protein Assay Kit (Pierce). For PrP^{Sc} detection, samples were digested with 40 μg/ml of proteinase K (PK; Sigma-Aldrich) at 37°C for 30 min, boiled for 5 min with SDS loading buffer (50 mM Tris-HCl pH 6.8, 5% glycerol, 1.6% SDS, 100 mM dithiothreitol), and subjected to SDS-PAGE. The proteins were transferred onto an Immobilon-P Membrane (Millipore) in transfer buffer containing 15% methanol at 300 mA for 90 min; the membrane was blocked with 5% nonfat dry milk in TBST (10 mM Tris-HCl pH 7.8, 100 mM NaCl, 0.1% Tween 20) for 30 min at room temperature and further incubated with primary antibodies. The immunoreactive bands were visualized using ECL Western Blotting Detection Kit (GE Healthcare Life Sciences).

Real-time PCR. Total RNA was isolated from cells using a TRIZOL® Reagent (Invitrogen). The first-strand cDNA was synthesized from 2 μg of total RNA with Super Script III Reverse Transcriptase (Invitrogen). The primers were: 5′-gctgccctatacccacatct-3′ and 5′-cgccttcatccgagaaac-3′ for p62 and 5′-aaatcgtgcgtgacatcaaa-3′ and 5′-aaggaaggctggaaaagagc-3′ for β-actin. β-actin mRNA was determined as a positive control. For real-time PCR, the synthesized cDNA was reacted with Fast Start Universal SYBR Green Master (Roche Applied Science) and measured by Light Cycler® 480 (Roche Applied Science).

Immunofluorescence analysis. Cells were fixed for 30 min at room temperature in 4% formaldehyde in PBS, permeabilized for 5 min at room temperature with 0.5% Triton X-100 in PBS, treated with 3 M guanidine thiocyanate for 5 min, blocked for 1 h at room temperature in TBST containing 5% skim milk, and incubated overnight at 4°C with the primary antibody in TBST containing 1% skim milk. After three washes in PBS, cells were incubated with the appropriate Alexa Fluor®-conjugated secondary antibodies (dilution 1 : 200) for 90 min at 37°C. For lysosomal staining, cells were stained with Lysotracker® dye (prepared according to kit instructions) for 30 min at 37°C. All images were obtained using a confocal laser-scanning microscope (Carl Zeiss).

Co-immunoprecipitation. ScN2a58 cells were grown to confluence in a 60 mm dish and treated with MG132 (10 μM, 24 h), and then harvested. Cells were lysed using cold immunoprecipitation lysis buffer (150 mM NaCl, 10 mM EDTA, 10 mM KH_2PO_4 pH 7.5) containing 2% Triton X-100. Cell debris was removed by centrifugation and the lysates were pre-cleaned for 30 min with protein G-Sepharose™ 4 Fast Flow (GE Healthcare Life Sciences). After the protein G-Sepharose was removed by centrifugation, the supernatant was incubated at 4°C with anti-p62 or anti-rabbit IgG antibodies for 2 h. Protein G-Sepharose was then added to the supernatant and incubation was continued for another 1 h. The immunoprecipitates were washed six times with washing buffer (150 mM NaCl, 10 mM Tris-HCl pH 7.4, 0.2% Tween-20), and resuspended in 2 × loading buffer.

In vivo infection experiments. Four-weeks-old ddY mice were purchased from SLC (Hamamatsu, Japan) and were intracerebrally inoculated with 20 μL of a 10^{-1}

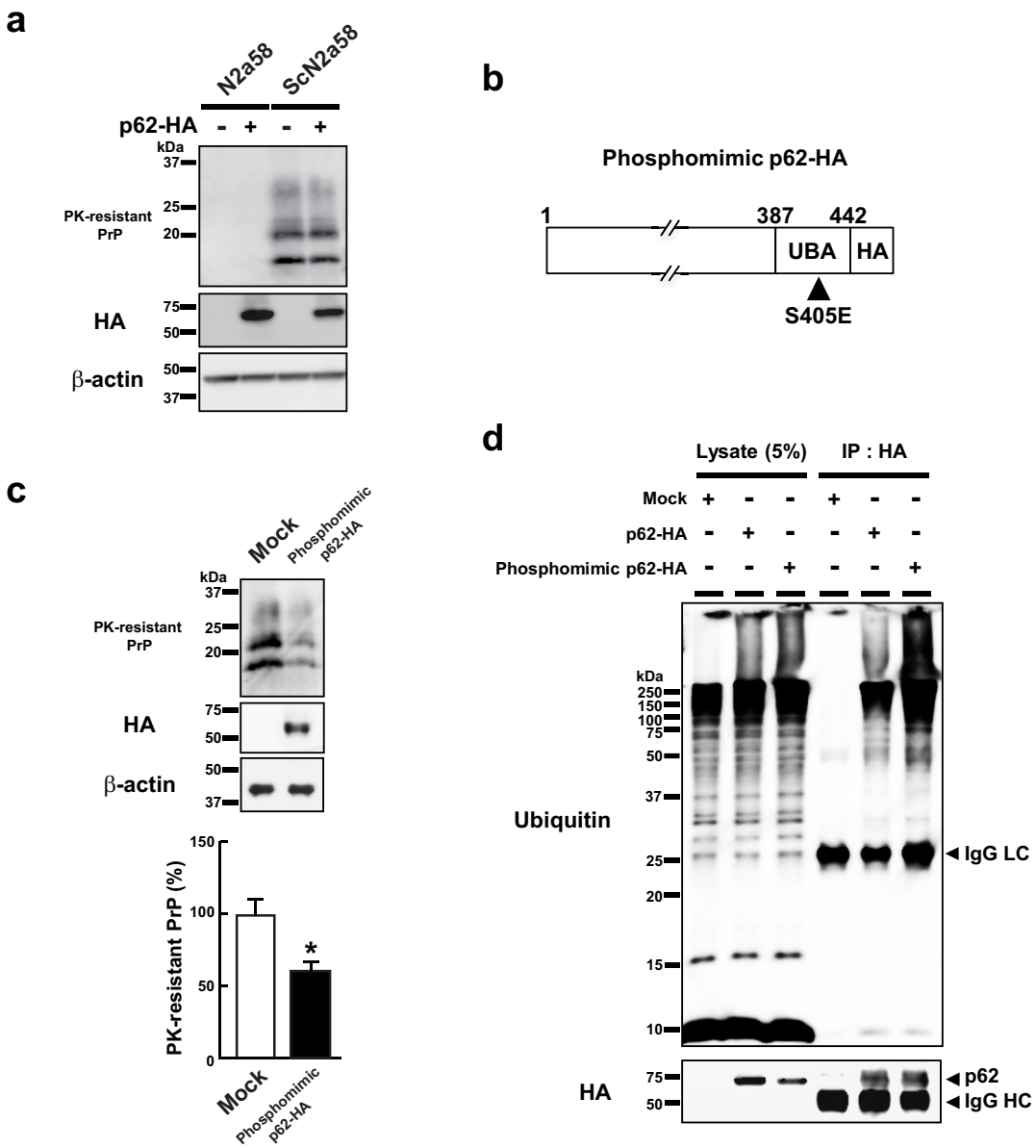

Figure 7 | Transient expression of phosphomimic p62 reduces the amount of PrP^{Sc}. (a) Mock or HA-tagged p62 expression vectors were transfected into N2a58 or ScN2a58 cells. The amount of PK-resistant PrP (M20) was analyzed by immunoblotting. The expression of transfected vectors was identified by anti-HA antibody. β-actin was used as a loading control. (b) Scheme of HA-tagged phosphomimic p62 (substitution of mouse p62 serine 405 for glutamate). (c) Mock or HA-tagged phosphomimic p62 expression vectors were transfected into ScN2a58 cells. The amount of PK-resistant PrP (M20) was analyzed by immunoblotting. The expression of transfected vectors was identified by anti-HA antibody. β-actin was used as a loading control. The amount of PK-resistant PrP was digitized and statistically analyzed using a two-tailed Student's *t*-test (*, $P < 0.01$). Data are presented as mean ± SD of three independent experiments. (d) Mock, HA-tagged p62, or phosphomimic p62 expression vectors were transfected into ScN2a58 cells. The lysates were then subjected to co-immunoprecipitation with anti-HA antibody, and blotted for anti-ubiquitin (top) and anti-HA (bottom) antibodies.

dilution of brain homogenate prepared from mice terminally sick with 22 L strain. As a control, age- and strain-matched mice were intracerebrally inoculated with phosphate buffered saline. The brains of the mice were removed at the terminal stage of disease. Animals were cared for in accordance with the Guidelines for Animal Experimentation of Nagasaki University.

1. Prusiner, S. B. Novel proteinaceous infectious particles cause scrapie. *Science* **216**, 136–144 (1982).
2. Bockman, J. M., Kingsbury, D. T., McKinley, M. P., Bendheim, P. E. & Prusiner, S. B. Creutzfeldt-Jakob disease prion proteins in human brains. *N. Engl. J. Med.* **312**, 73–78 (1985).
3. Prusiner, S. B. *et al.* Scrapie prions aggregate to form amyloid-like birefringent rods. *Cell* **35**, 349–358 (1983).
4. Arrasate, M., Mitra, S., Schweitzer, E. S., Segal, M. R. & Finkbeiner, S. Inclusion body formation reduces levels of mutant huntingtin and the risk of neuronal death. *Nature* **431**, 805–810 (2004).
5. Kristiansen, M. *et al.* Disease-associated prion protein oligomers inhibit the 26S proteasome. *Mol. Cell* **26**, 175–188 (2007).
6. Rubinsztein, D. C. The roles of intracellular protein-degradation pathways in neurodegeneration. *Nature* **443**, 780–786 (2006).
7. Bennett, E. J., Bence, N. F., Jayakumar, R. & Kopito, R. R. Global impairment of the ubiquitin-proteasome system by nuclear or cytoplasmic protein aggregates precedes inclusion body formation. *Mol. Cell* **17**, 351–365 (2005).
8. Garcia-Mata, R., Gao, Y. S. & Sztul, E. Hassles with taking out the garbage: aggravating aggresomes. *Traffic* **3**, 388–396 (2002).
9. Johnston, J. A., Ward, C. L. & Kopito, R. R. Aggresomes: a cellular response to misfolded proteins. *J. Cell Biol.* **143**, 1883–1898 (1998).
10. Johnston, J. A., Illing, M. E. & Kopito, R. R. Cytoplasmic dynein/dynactin mediates the assembly of aggresomes. *Cell Motil. Cytoskelet.* **53**, 26–38 (2002).
11. Bjørkøy, G. *et al.* p62/SQSTM1 forms protein aggregates degraded by autophagy and has a protective effect on huntingtin-induced cell death. *J. Cell Biol.* **171**, 603–614 (2005).

12. Ichimura, Y. *et al.* Structural basis for sorting mechanism of p62 in selective autophagy. *J. Biol. Chem.* **283**, 22847–22857 (2008).
13. Komatsu, M. *et al.* Homeostatic levels of p62 control cytoplasmic inclusion body formation in autophagy-deficient mice. *Cell* **131**, 1149–63 (2007).
14. Pankiv, S. *et al.* p62/SQSTM1 binds directly to Atg8/LC3 to facilitate degradation of ubiquitinated protein aggregates by autophagy. *J. Biol. Chem.* **282**, 24131–24145 (2007).
15. Iwata, A., Riley, B. E., Johnston, J. A. & Kopito, R. R. HDAC6 and microtubules are required for autophagic degradation of aggregated huntingtin. *J. Biol. Chem.* **280**, 40282–40292 (2005).
16. Pandey, U. B. *et al.* HDAC6 rescues neurodegeneration and provides an essential link between autophagy and the UPS. *Nature* **447**, 859–863 (2007).
17. Babu, J. R., Geetha, T. & Wooten, M. W. Sequestosome 1/p62 shuttles polyubiquitinated tau for proteasomal degradation. *J. Neurochem.* **94**, 192–203 (2005).
18. Kuusisto, E., Suuronen, T. & Salminen, A. Ubiquitin-binding protein p62 expression is induced during apoptosis and proteasomal inhibition in neuronal cells. *Biochem. Biophys. Res. Commun.* **280**, 223–228 (2001).
19. Nakano, T., Nakaso, K., Nakashima, K. & Ohama, E. Expression of ubiquitin-binding protein p62 in ubiquitin-immunoreactive intraneuronal inclusions in amyotrophic lateral sclerosis with dementia: analysis of five autopsy cases with broad clinicopathological spectrum. *Acta Neuropathol.* **107**, 359–364 (2004).
20. Nakaso, K. *et al.* Transcriptional activation of p62/A170/ZIP during the formation of the aggregates: possible mechanisms and the role in Lewy body formation in Parkinson's disease. *Brain Res.* **1012**, 42–51 (2004).
21. Tanji, K. *et al.* p62/sequestosome 1 binds to TDP-43 in brains with frontotemporal lobar degeneration with TDP-43 inclusions. *J. Neurosci. Res.* **000**, 1–9 (2012).
22. Zatloukal, K. *et al.* p62 Is a common component of cytoplasmic inclusions in protein aggregation diseases. *Am. J. Pathol.* **160**, 255–263 (2002).
23. Aguib, Y., Heiseke, A., Gilch, S. & Riemer, C. Autophagy induction by trehalose counteracts cellular prion infection. *Autophagy* 361–369 (2009).
24. Heiseke, A., Aguib, Y., Riemer, C., Baier, M. & Schatzl, H. M. Lithium induces clearance of protease resistant prion protein in prion-infected cells by induction of autophagy. *J. Neurochem.* **109**, 25–34 (2009).
25. Nakagaki, T. *et al.* FK506 reduces abnormal prion protein through the activation of autolysosomal degradation and prolongs survival in prion-infected mice. *Autophagy* **9**, 1–9 (2013).
26. Ma, J. & Lindquist, S. Wild-type PrP and a mutant associated with prion disease are subject to retrograde transport and proteasome degradation. *Proc. Natl. Acad. Sci. U S A* **98**, 14955–14960 (2001).
27. Yedidia, Y., Horonchik, L., Tzaban, S., Yanai, A. & Taraboulos, A. Proteasomes and ubiquitin are involved in the turnover of the wild-type prion protein. *EMBO J.* **20**, 5383–5391 (2001).
28. Drisaldi, B. *et al.* Mutant PrP is delayed in its exit from the endoplasmic reticulum, but neither wild-type nor mutant PrP undergoes retrotranslocation prior to proteasomal degradation. *J. Biol. Chem.* **278**, 21732–43 (2003).
29. Fioriti, L. *et al.* Cytosolic prion protein (PrP) is not toxic in N2a cells and primary neurons expressing pathogenic PrP mutations. *J. Biol. Chem.* **280**, 11320–8 (2005).
30. Rane, N. S., Yonkovich, J. L. & Hegde, R. S. Protection from cytosolic prion protein toxicity by modulation of protein translocation. *EMBO J.* **23**, 4550–9 (2004).
31. Shin, J. P62 and the sequestosome, a novel mechanism for protein metabolism. *Arch. Pharm. Res.* **21**, 629–633 (1998).
32. Taraboulos, A., Serban, D. & Prusiner, S. B. Scrapie prion proteins accumulate in the cytoplasm of persistently infected cultured cells. *J. Cell Biol.* **110**, 2117–2132 (1990).
33. Seibenhener, M. L. *et al.* Sequestosome 1/p62 Is a Polyubiquitin Chain Binding Protein Involved in Ubiquitin Proteasome Degradation. *Mol. Cell. Biol.* **24**, 8055–8068 (2004).
34. Matsumoto, G., Wada, K., Okuno, M., Kurosawa, M. & Nukina, N. Serine 403 Phosphorylation of p62/SQSTM1 Regulates Selective Autophagic Clearance of Ubiquitinated Proteins. *Mol. Cell* **44**, 279–289 (2011).
35. Xu, Y. *et al.* Activation of the macroautophagic system in scrapie-infected experimental animals and human genetic prion diseases. *Autophagy* **8**, 1604–1620 (2012).
36. Ishii, T. *et al.* Low micromolar levels of hydrogen peroxide and proteasome inhibitors induce the 60-kDa A170 stress protein in murine peritoneal macrophages. *Biochem. Biophys. Res. Commun.* **232**, 33–37 (1997).
37. Deriziotis, P. *et al.* Misfolded PrP impairs the UPS by interaction with the 20S proteasome and inhibition of substrate entry. *EMBO J.* **30**, 3065–3077 (2011).
38. Jain, A. *et al.* p62/SQSTM1 is a target gene for transcription factor NRF2 and creates a positive feedback loop by inducing antioxidant response element-driven gene transcription. *J. Biol. Chem.* **285**, 22576–22591 (2010).
39. Yamamoto, N. *et al.* Proteasome inhibition induces glutathione synthesis and protects cells from oxidative stress: relevance to Parkinson disease. *J. Biol. Chem.* **282**, 4364–72 (2007).
40. Komatsu, M. *et al.* The selective autophagy substrate p62 activates the stress responsive transcription factor Nrf2 through inactivation of Keap1. *Nat. Cell Biol.* **12**, 213–223 (2010).
41. Ironside, J. W., McCardle, L., Hayward, P. A. & Bell, J. E. Ubiquitin immunocytochemistry in human spongiform encephalopathies. *Neuropathol. Appl. Neurobiol.* **19**, 134–140 (1993).
42. Kovacs, G. G., Preusser, M., Strohschneider, M. & Budka, H. Subcellular localization of disease-associated prion protein in the human brain. *Am. J. Pathol.* **166**, 287–294 (2005).
43. Watanabe, Y. *et al.* p62/SQSTM1-dependent autophagy of Lewy body-like alpha-synuclein inclusions. *PLoS One* **7**, e52868 (2012).
44. Doi, H. & Adachi, H. p62/SQSTM1 differentially removes the toxic mutant androgen receptor via autophagy and inclusion formation in a spinal and bulbar muscular atrophy mouse model. *J. Neurosci.* **33(18)**, 7710–7727 (2013).
45. Xu, Y. *et al.* Overexpression of p62/SQSTM1 promotes the degradations of abnormally accumulated PrP mutants in cytoplasm and relieves the associated cytotoxicities via autophagy-lysosome-dependent way. *Med. Microbiol. Immunol.* (2013). doi:10.1007/s00430-013-0316-z.
46. Atarashi, R., Sim, V. L., Nishida, N., Caughey, B. & Katamine, S. Prion strain-dependent differences in conversion of mutant prion proteins in cell culture. *J. Virol.* **80**, 7854–62 (2006).
47. Nishida, N. *et al.* Successful transmission of three mouse-adapted scrapie strains to murine neuroblastoma cell lines overexpressing wild-type mouse prion protein. *J. Virol.* **74**, 320–325 (2000).
48. Iwamaru, Y. *et al.* Microglial cell line established from prion protein-overexpressing mice is susceptible to various murine prion strains. *J. Virol.* **81**, 1524–1527 (2007).
49. Ishibashi, D. *et al.* Protective role of interferon regulatory factor 3-mediated signaling against prion infection. *J. Virol.* **86**, 4947–4955 (2012).

Acknowledgments

This work was supported by a grant-in aid for science research (B: grant no. 23300127, C: grant no. 24591482) from the Ministry of Education, Culture, Sports, Science, and Technology of Japan; a grant-in-aid of the Research Committee of Prion disease and Slow Virus Infection, from the Ministry of Health, Labor and Welfare of Japan; a grant from Takeda Science Foundation. This work was also supported by a grant for Japan Intractable Disease Research Foundation, and was also supported in a part by a Grant-in-Aid from the Tokyo Biochemical Research Foundation.

Author contributions

T.H. designed the work, produced all the data, and wrote the manuscript. T.N., K.Satoh and K.Sano contributed reagents and materials. D.I., R.A. and N.N. revised the manuscript.

Additional information

Supplementary information accompanies this paper at http://www.nature.com/scientificreports

Competing financial interests: The authors declare no competing financial interests.

How to cite this article: Homma, T. *et al.* Increased expression of p62/SQSTM1 in prion diseases and its association with pathogenic prion protein. *Sci. Rep.* **4**, 4504; DOI:10.1038/srep04504 (2014).